A MULTIRESOLUTION DIRECTIONAL OPERATOR FOR SIDESCAN SONAR IMAGE ANALYSIS

D R Carmichael (1), L M Linnett (2), S J Clarke (2)

(1) Defence Research Agency, Newton's Road, Weymouth, Dorset
(2) Department of Computing & Electrical Engineering, Heriot-Watt University, Riccarton, Edinburgh

1. INTRODUCTION

This paper presents a multiresolution operator for the analysis of ground truthed sidescan sonar images, the origins of which lie in the body of fractal theory. Results are presented for the classification of individual groundtruthed sediments and the segmentation of composite images containing these sediments using both linear and quadratic maximum likelihood supervised classification schemes. The improvement which may be obtained by employing directional as opposed to isotropic features is demonstrated. The results show excellent classification and segmentation accuracy. Six sediment types were analysed, namely clay, mud, rock, stones, sand and gravel. The method shows promising results for improved swathe seabed classification.

2. BACKGROUND

In recent years the improvement in quality of sidescan sonar has lead to the production of image quality data. This data is often required for seabed classification purposes. In 1988 Pace and Gao [1] proposed a scheme for swathe seabed classification using sidescan sonar. This method was based on features obtained from the bottom-backscatter (which comprises a two dimensional textural signal). Recently several other attempts, also based on these features, have been presented, for example Tamsett [2], and Edgecock [3]. Maguire and Pace [4] have recently modified these features with improved results. Essentially the methods consist of measuring parameters obtained from the power spectrum in the across track direction. Improved estimates are obtained by averaging in the along track direction. While good results are obtained for separate images of individual sediments the necessary size of the sample window used to obtained the power spectra estimates precludes accurate delineation of boundaries between sediments.

In this paper the authors propose a new technique based on fractal measures of roughness of the sediments and show that improved classification accuracy together with excellent segmentation performance may be obtained. The measures are based on an original idea of Peleg *et al.* [5] who showed that these features capture phase as well as magnitude information without the need for traditional Fourier techniques. The idea of a directional fractal dimension was postulated but not taken further. The authors [6] have previously exploited directionality for photographic textures [7] and in the present paper they show that, using a fractal method based on Peleg's technique, excellent classification and segmentation results for sidescan sonar images of sediments may be achieved.

The authors explore the use of asymmetry and directionality for local fractal measures. In this technique the fractal dimension is obtained by local averaging about a given pixel location. The fractal dimension is computed over a range of octave scale ranges in different directions to provide a set of feature values. These are then input to Fisher's linear and quadratic discriminants [8] from which a classification/segmentation is obtained. The analysis is performed on the same dataset of sediments as used by previous authors [1][2][3][4] in order to provide a comparison between the techniques. Six sediments were analysed:- clay, mud, rock, stones, gravel and sand.

3. THEORY

Fractal dimension may be determined by measuring the change in surface area of the texture with scale. A variant on the method of Peleg *et al.* [5] for the measurement of fractal dimension has been shown by the authors [6] to give good texture segmentation results. Consider all points with distances to the surface of no more than ε. These points form an upper and lower surface of width 2ε between them. The suggested area between the two *blanket* surfaces is the volume enclosed, divided by 2ε. As ε decreases the area, A_ε, increases. It is the rate of change of this area with scale, ε, which determines the fractal dimension. For a pure fractal the rate of change of area with scale is constant. In practice, however, for many naturally occurring textures this rate of change of surface area is not constant over all scales. This is an important factor which is exploited in this paper.

3.1 Computation of Upper and Lower Surfaces

For ease of notation a one dimensional signal is considered first. The case for a two dimensional surface ie image follows from this. Consider a signal $g(x)$. The upper and lower blankets, $u_\varepsilon(x)$ and $b_\varepsilon(x)$, at distance ε, above and below the signal may be computed as

$$u_\epsilon(x) = \max_i \left\{ g(x+i) + \epsilon - |i| \right\} \qquad \forall\, i \in \{-\epsilon,\ldots,0,\ldots,\epsilon\} \tag{4}$$

and

$$b_\epsilon(x) = \min_i \left\{ g(x+i) - \epsilon + |i| \right\} \qquad \forall\, i \in \{-\epsilon,\ldots,0,\ldots,\epsilon\} \tag{5}$$

respectively. The extension to two dimensional image data, $g(x,y)$, is straight forward leading to the following forms for direct computation of the upper and lower blankets respectively:

$$u_\epsilon(x,y) = \max_{i,j} \left\{ g(x+i,y+j) + \epsilon - \max\{|i|,|j|\} \right\} \qquad \forall\, i,j \in \{-\epsilon,\ldots,0,\ldots,\epsilon\}$$

$$b_\epsilon(x,y) = \min_{i,j} \left\{ g(x+i,y+j) - \epsilon + \max\{|i|,|j|\} \right\} \tag{6),(7}$$

Recursive forms are also readily derived which are consistent with the above.

3.2 Estimation of Fractal Dimension

For a fractal surface the blanket area, A_ε, at distance ε above or below the surface obeys the relationship, [9],

$$A_\epsilon = F\epsilon^{2-D}$$

where F is a constant and D is the fractal dimension. Thus, given two blankets at distances ε_2 and ε_1 from the original surface the fractal dimension may be obtained as

$$D_{\epsilon_2,\epsilon_1} = 2 - \frac{(\ln A_{\epsilon_2} - \ln A_{\epsilon_1})}{(\ln\epsilon_2 - \ln\epsilon_1)} \tag{8}$$

If the surface is fractal then the value obtained for D will be independent of the distances ε_2 and ε_1 at which the blankets are computed. In practice, however, many naturally occurring textures cannot be considered truly fractal over the range of scales used and we therefore retain the explicit reference to ε_2 and ε_1 within the above definition to indicate that the value obtained for D is a function of the blanket areas at both ε_2 and ε_1. In practice the fractal dimension at a given pixel location, (m,n), must be estimated from a finite set of samples taken about that location. The local surface area for each point is obtained by measuring the volume enclosed between the upper and lower blankets within a $(2L+1)*(2L+1)$ window region centred on that pixel location according to

$$A_\epsilon(m,n) = \frac{V_\epsilon(m,n)}{2\epsilon}$$

where the volume, $V_\varepsilon(m,n)$, is obtained from

$$V_\epsilon(m,n) = \sum_{x,y}\left(u_\epsilon(x,y) - b_\epsilon(x,y)\right) \qquad \begin{array}{l} \forall\, x \in \{m-L,\ldots,m+L\} \\ \forall\, y \in \{n-L,\ldots,n+L\} \end{array} \tag{9}$$

Substituting (9) into (8) we estimate the fractal dimension at pixel location (m,n) as

$$\hat{D}_{\epsilon_2,\epsilon_1}(m,n) = 3 - \frac{(\ln V_{\epsilon_2}(m,n) - \ln V_{\epsilon_1}(m,n))}{(\ln\epsilon_2 - \ln\epsilon_1)} \tag{10}$$

Figure 1 shows the average fractal dimension computed using (6) and (7) in (10) over a range of scales for each of the six sediments. As may be seen these cannot be considered truly fractal over the 4 octave range of scales which was used to generate the blankets. In fact there is a wide variation in the local fractal dimension with values ranging from just over 2.1 to a maximum of approximately 2.7. The variability of the measurements would suggest that fractal dimension as estimated over a range of different scales may be a useful feature for discrimination purposes and would provide more discriminatory power, for these naturally occurring textures, than a single fractal dimension estimate computed over the entire scale range. However, the similarity between the curves suggests that the discrimination using this measure alone may only achieve limited success.

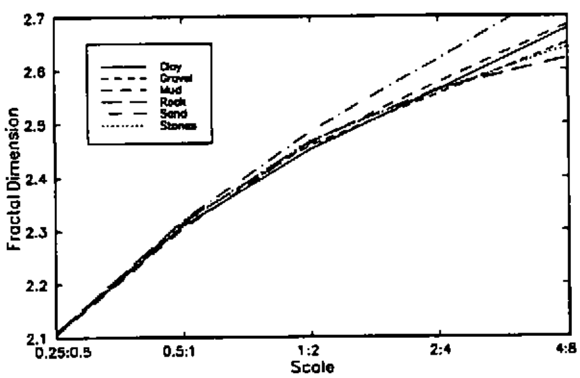

Figure 1. Variation in fractal dimension with scale, six sediments

3.3 Asymmetry

As pointed out by Peleg *et al.* [5] some textures are found to exhibit asymmetry in that the upper and lower blankets may not necessarily share the same characteristics. The authors [6] have shown that this asymmetry can be used to advantage to improve texture discrimination. Thus, rather than estimating blanket area from the volume enclosed between both the upper and lower surfaces, it is possible to exploit any asymmetry which may be present by calculating two different blanket areas, $A_\epsilon^+(m,n)$ and $A_\epsilon^-(m,n)$, according to

$$A_\epsilon^\pm(m,n) = \frac{V_\epsilon^\pm(m,n)}{\epsilon}$$

where the volumes contained between the texture surface and the upper and lower blankets are given by

$$V^+_\epsilon(m,n) = \sum_{x,y}\left(u_\epsilon(x,y) - g(x,y)\right) \tag{11}$$

and

$$V^-_\epsilon(m,n) = \sum_{x,y}\left(g(x,y) - b_\epsilon(x,y)\right) \tag{12}$$

respectively. Equations (11) and (12) are employed within (10) to derive two estimates of fractal dimension at each pixel location.

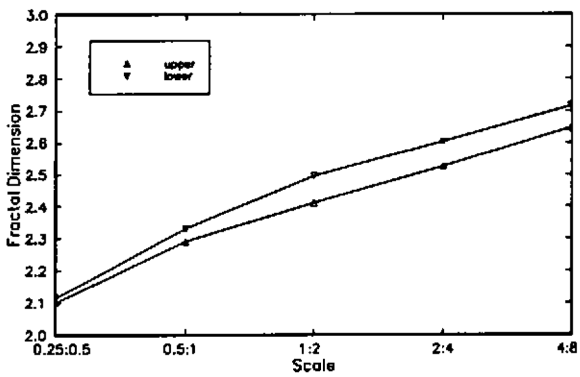

(a) Clay

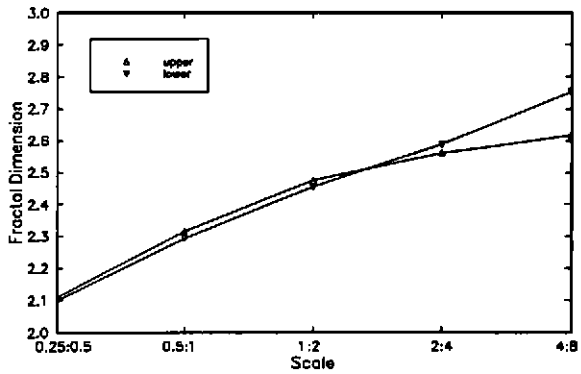

(b) Mud

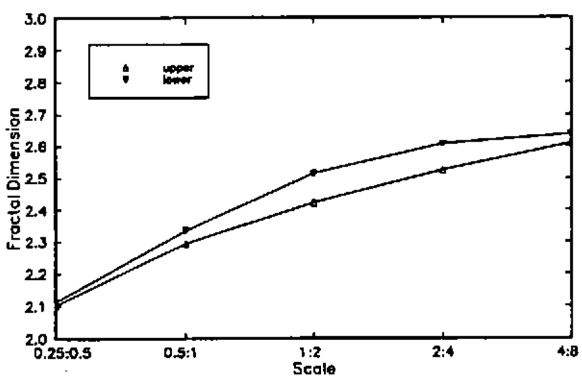

(c) Rock

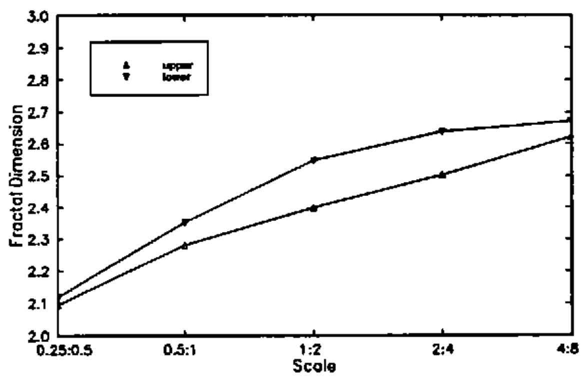

(d) Stones

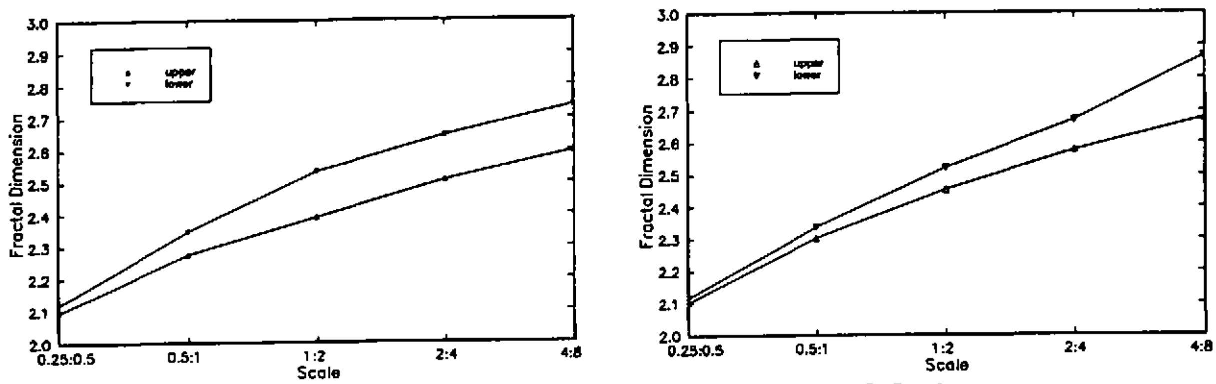

(e) Gravel (f) Sand

Figure 2. Asymmetry, variation in fractal dimension with scale.

Figure 2 shows estimates of fractal dimension for each of the six sediments. In this case, however, both the upper and lower blankets are used separately to obtain the estimates. Whereas previously there was very little difference between the sediments, particularly over the smaller scale ranges, it is now seen that, with the exception of mud, marked differences exist between the fractal dimension measures as computed from either the upper or lower blankets. This is further evidence that such sediments are not truly fractal and is a useful property which may be exploited during the feature generation stage prior to classification.

3.4 Directionality

Since many textures exhibit directional characteristics it would be advantageous to use this property in deriving the features which are to be used for classification. This is readily achieved by altering the manner in which the blankets are computed. Thus, rather than examining all pixels in the neighbourhood of a given pixel, as in equations (6) and (7), we now examine only those points which lie in specific directions relative to the current pixel of interest. This is achieved by examining transects through the image in four different directions 0°, 45°, 90°, and 135° each pixel location. Thus, for example, the four directional upper blankets are now computed as

$$
\begin{aligned}
u_\epsilon^{(1)}(x,y) &= \max_i \left\{ g(x+i,y) + \epsilon - |i| \right\} \qquad \forall\, i \in \{-\epsilon,\ldots,0,\ldots,\epsilon\} \\
u_\epsilon^{(2)}(x,y) &= \max_i \left\{ g(x+i,y-i) + \epsilon - |i| \right\} \\
u_\epsilon^{(3)}(x,y) &= \max_i \left\{ g(x,y+i) + \epsilon - |i| \right\} \\
u_\epsilon^{(4)}(x,y) &= \max_i \left\{ g(x+i,y+i) + \epsilon - |i| \right\}
\end{aligned}
\qquad (13)
$$

where the superscripts (1), (2), (3), and (4) denote directions 0°, 45°, 90°, and 135° respectively. Similar relationships exist for the lower blankets. Figure 3 shows the results obtained for gravel and mud, respectively, using measures (1) to (4) with both upper and lower blankets. The fractal dimension estimates show that both gravel and mud exhibit different characteristics in different directions. This was also found to be the case for the remaining sediments in the data set. The fractal dimension measured in the across track direction (0°) was also found to differ considerably from that in any of the three remaining directions. This is particularly evident for mud as shown in figure 3b. This might be explained by the fact that the across track resolution is typically much better than the along track resolution for sidescan sonar systems. Gravel exhibits some degree of asymmetry in all directions, particularly at the larger scales. This was also found, generally, to be true of the remaining sediments in the dataset with the exception of mud which shows negligible difference between upper and lower fractal dimension estimates.

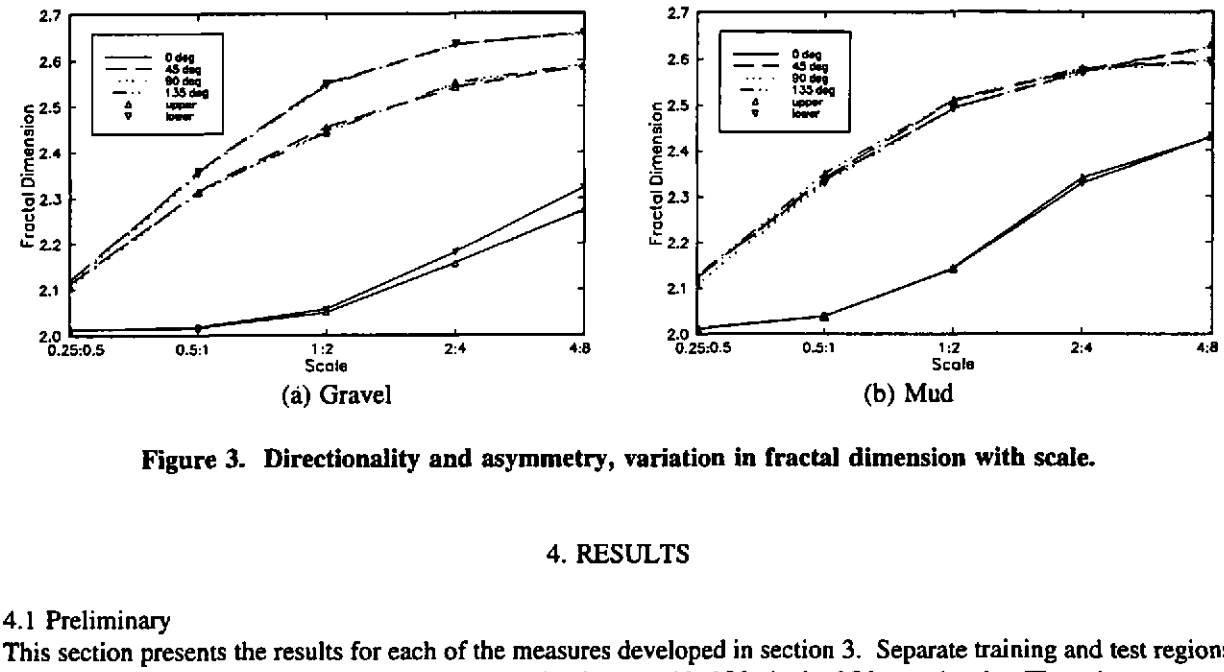

(a) Gravel

(b) Mud

Figure 3. Directionality and asymmetry, variation in fractal dimension with scale.

4. RESULTS

4.1 Preliminary

This section presents the results for each of the measures developed in section 3. Separate training and test regions were chosen for all sediments. The images examined were 128*256 pixels, 256 grey levels. These images were part of the data set used by Pace and Gao [1].

4.2 Classification

For all the results presented in this section point estimates, measured over a 29*29 window, were used as features for both linear and quadratic discriminants. The features were estimated over 3 octaves. Twelve images comprising six sediments as shown in figure 4, were selected. These are, from left to right and top to bottom, clay03, clay04, mud02, mud01, rock01, rock02, stones02, stones01, gravel03, gravel04, sand03, sand04. It was suggested, in section 3.2., that the fractal dimension be obtained from the volume enclosed between upper and lower blankets. Point estimates of the fractal dimension based on the difference between blankets were computed using equations (6) and (7) ie assuming anisotropy within the textures. Table 1 shows the contingency table for the results of this classification. The average correct classification for the quadratic discriminant shown in table 1 is 80.69%. A similar result is obtained for the linear discriminant its average being 75.31%. Evidence was presented in section 3.3 suggesting that asymmetry between upper and lower blankets could give improved discrimination. Estimating fractal dimension by computing volumes using equations (11) and (12) again produces point estimates but this time taking the asymmetry into account. Table 2 shows the equivalent results for the same six sediments. The average correct classification for the quadratic discriminant shown in table 2 is 96.00%. A similar result is obtained for the linear discriminant its average being 93.31%. An examination of tables 1 and 2 shows that there is a significant improvement in classification success rate by taking into account asymmetry between upper and lower blankets.

	Clay	Mud	Rock	Stones	Gravel	Sand
Clay	53.91	14.01	0.00	16.84	15.19	0.05
Mud	24.49	64.59	0.00	5.68	2.81	2.43
Rock	0.00	0.00	97.46	2.54	0.00	0.00
Stones	3.15	0.60	1.52	94.73	0.00	0.00
Gravel	7.74	14.29	0.00	0.48	71.91	5.58
Sand	0.00	1.17	0.00	0.00	0.28	98.55

Table 1. Percentage correct classification, no directionality, no asymmetry, quadratic discriminant.

	Clay	Mud	Rock	Stones	Gravel	Sand
Clay	90.60	6.25	0.00	0.14	2.57	0.44
Mud	2.98	95.48	0.00	0.00	0.00	1.54
Rock	0.00	0.00	96.93	3.07	0.00	0.00
Stones	1.12	0.00	1.19	97.69	0.00	0.00
Gravel	3.60	0.20	0.00	0.00	95.72	0.48
Sand	0.04	0.40	0.00	0.00	0.00	99.56

Table 2. Percentage correct classification, no directionality, with asymmetry, quadratic discriminant.

In section 3.4 fractal dimension measures incorporating directionality, (equation (12)), were proposed. Again, qualitative evidence was presented suggesting that this was an important characteristic which could be used for enhanced discrimination. Table 3 shows the results using the four directions as in equation (12).

	Clay	Mud	Rock	Stones	Gravel	Sand
Clay	98.25	1.68	0.00	0.00	0.00	0.07
Mud	0.59	99.27	0.00	0.00	0.00	0.14
Rock	0.07	0.00	99.57	0.36	0.00	0.00
Stones	0.13	0.00	0.00	99.41	0.17	0.29
Gravel	0.11	0.00	0.00	0.04	99.84	0.01
Sand	0.05	0.07	0.00	0.00	0.00	99.88

Table 3. Percentage correct classification, with directionality and asymmetry, quadratic discriminant.

The average correct classification, over all twelve textures, is 99.37%. The linear discriminant yielded an average of 99.2%. The evidence then is that improved classification may be obtained by utilising asymmetry and directionality in deriving fractal dimension feature measures. The average correct classification was improved from

80.69% to 96.0% by introducing asymmetry and to 99.37% by further use of directionality.

4.3 Segmentation

As a further example of the discrimination ability of the measures a composite image was formed from all of the twelve examples of the six sediments. This image is shown in figure 4. Table 4 is a schematic representation of the ground truth image showing the locations of the various sediments within the image.

Clay03	Clay04
Mud02	Mud01
Rock01	Rock02
Stones02	Stones01
Gravel03	Gravel04
Sand03	Sand04

Table 4. Schematic of sediments in original image.

Figure 4. Original image.

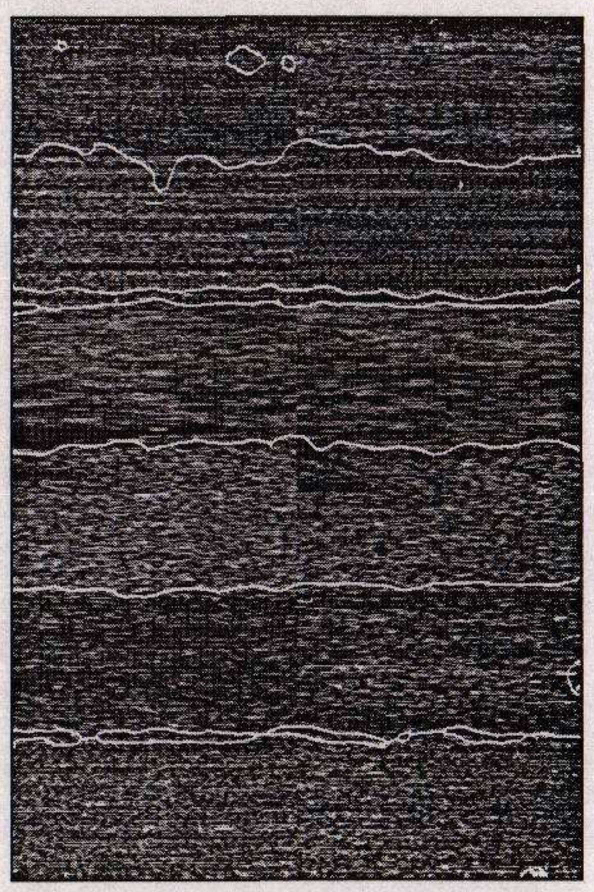

Figure 5. Segmented overlaid image.

Each individual sediment is represented by an image of size 128*256 making the total image 768*512 pixels. Using the four directions and asymmetry measures point estimates of the fractal dimension were obtained and used to classify each pixel of the image. The result shown overlaid on the original is presented in figure 5. As can be seen an excellent segmentation is achieved.

5. CONCLUSIONS

A set of features based on estimates of fractal dimension has been proposed. It was shown that the use of asymmetry in the estimation of fractal dimension was a useful discriminator between sediments. The discrimination was further enhanced by the incorporation of directional estimates. An average success rate of 99.37% for six sediments was achieved using a supervised classification scheme. It was shown that this classification system could be applied successfully to segmentation of a composite image of these sediments. This suggests that this technique may have important applications with regard to seabed mapping and hydrography.

6. ACKNOWLEDGEMENTS

The authors wish to express thanks to Dr. N.G.Pace for kindly supplying a set of the data from his work in [1].

7. REFERENCES

[1] N.G.Pace, H.Gao, 'Swathe Seabed Classification', IEEE Journal of Oceanic Engineering, Vol.13, 2, pp83-90, 1988.

[2] D.Tamsett, 'Seabed Characterisation and Classification from the Power Spectra of Sidescan Sonar Data', Marine Geophysical Researches, Vol15, pp43-64, 1993.

[3] T.M.Edgecock, 'Towards Gain Invariant Sea Bed Classification', Proc. I.O.A, Vol 16, Part 6, pp217-224, 1994.

[4] P.M.Maguire, N.G.Pace, 'Swathe Seabed Classification', Personal Communication.

[5] S.Peleg, J.Naor, R.Hartley, D.Avnir, 'Multiple Resolution Texture Analysis and Classification', IEEE Transactions on Pattern Analysis and Machine Intelligence, Vol. PAMI-6, No.4, pp518-523, July 1984.

[6] L.M.Linnett, D.R.Carmichael, S.J,Clarke, 'A Multiresolution Directional Operator for Texture Analysis', Submitted to Pattern Recognition, June, 1995.

[7] P.Brodatz, 'Textures - A Photographic Album for Artists and Designers', Dover, New York, 1966.

[8] M.James, 'Classification Algorithms', Collins, London, 1985.

[9] B.B.Mandelbrot, 'The Fractal Geometry of Nature', W.H.Freeman, New York, 1983.